

KCO1 is a component of the slow-vacuolar (SV) ion channel

Gerald Schönknecht^{a,c,1}, Petra Spoormaker^{b,1}, Ralf Steinmeyer^a, Liubov Brüggeman^a,
Peter Ache^a, Rajiv Dutta^c, Birgit Reintanz^b, Matthias Godde^b, Rainer Hedrich^a,
Klaus Palme^{b,*}

^aJulius-von-Sachs-Institut für Biowissenschaften, Lehrstuhl für Molekulare Pflanzenphysiologie und Biophysik, Universität Würzburg, Julius-von-Sachs-Platz 2, 97082 Würzburg, Germany

^bMax-Delbrück-Laboratorium in der Max-Planck-Gesellschaft, Carl-von-Linné Weg 10, 50829 Cologne, Germany

^cDepartment of Botany, Oklahoma State University, 104 Life Sciences East, Stillwater, OK 74078, USA

Received 11 October 2001; revised 5 December 2001; accepted 5 December 2001

First published online 14 December 2001

Edited by Felix Wieland

Abstract The *Arabidopsis* double pore K⁺ channel KCO1 was fused to green fluorescent protein and expressed in tobacco protoplasts. Microscopic analysis revealed a bright green fluorescence at the vacuolar membrane. RT-PCR experiments showed that KCO1 is expressed in the mesophyll. Vacuoles from *Arabidopsis* wild-type and *kco1* knockout plants were isolated for patch-clamp analyses. Currents mediated by slow-activating vacuolar (SV) channels of mesophyll cell vacuoles were significantly smaller in *kco1* plants compared to the wild-type. This shows that KCO1 is involved in the formation of SV channels. © 2002 Published by Elsevier Science B.V. on behalf of the Federation of European Biochemical Societies.

Key words: Two-pore domain K⁺ channel;
Vacuolar membrane; Patch-clamp;
Green fluorescence protein; *Arabidopsis thaliana*

1. Introduction

Since the cloning and functional expression of the first plant ion channels [1,2] at least five different K⁺ channel gene families have been identified in *Arabidopsis thaliana*. They structurally separate into the ‘shaker-like’ (six transmembrane domains and one pore: S₆P₁), the ‘two-pore’ (S₄P₂) and the Kir-type (S₂P₁) K⁺ channels [3]. To understand the physiological function of the corresponding gene products, knowledge of the subcellular localization of expressed ion channels is essential. Up to now, the subcellular localization of only a few K⁺ channels has been analyzed [4,5] and they all represent plasma membrane channels. Electrophysiological studies, however, revealed ion channels not only in the plasma membrane but also in the membrane of organelles (e.g. vacuole [6], ER [7], and chloroplast [8]). In the vacuolar membrane, which encloses the largest cellular compartment, at least three cation channels have been identified: the slow-activating vacuolar (SV) channel, fast-activating vacuolar (FV) channel and vacuolar potas-

sium channel (VK) channel. The SV channel is activated by cytosolic Ca²⁺ and positive voltages [6,9]. The SV channel is permeable for mono- as well as divalent cations [10,11] and seems to be ubiquitous in all terrestrial plants (*Embryophyta*) [12]. The FV channel opens at positive voltages, is selective for monovalent cations [13] and blocked by divalent cations [6,14]. The VK channel is K⁺-selective, voltage-independent, activated by Ca²⁺ and has so far been observed in guard cells only [11,15]. Up to now, nothing is known about the molecular nature of these ion channels.

Recently, in plants the first member of the new and rapidly growing class of two-pore K⁺ channels was identified and named KCO1 for K⁺ channel outward rectifying. KCO1 was cloned from *A. thaliana* and was found to be expressed at low levels in leaves, seedling, and flowers [16]. When expressed in insect cells, slow-activating, outward rectifying K⁺ currents with a very steep Ca²⁺ dependency could be measured. Based on its appearance in the plasma membrane of KCO1-expressing insect cells, it was assumed that KCO1 represents a plasma membrane outward rectifying K⁺ channel [16]. In the present study we demonstrate, however, that KCO1–green fluorescent protein (GFP) fusion proteins expressed in tobacco BY2 cells are targeted predominantly to the vacuolar membrane. KCO1 is expressed in mesophyll cells at a relative high level. By patch-clamp analyses on *Arabidopsis* mesophyll vacuoles we show that SV channel currents are decreased in plants carrying an *En-1* insertion in the KCO1 gene.

2. Material and methods

2.1. Construction of the GFP fusion protein

For the construction of the KCO1–GFP fusion, KCO1 cDNA was amplified by PCR using pBluescript KCO1 (P.S., Ph.D. Thesis, University Cologne, Germany) as a template. The forward primer (5'-AGA CTC GAG GCA TCC ATG TCT TCG G-3') contains a *Xho*I site and the reverse primer (5'-AGG TGA CAT GTA CCT TTG AAT CTG AGA CG-3'), a *Bsp*LU111 site, and mutated the KCO1 stop codon TAA to TAC. The isolated PCR fragment was digested with *Xho*I and *Bsp*LU111 and the resulting 743-bp fragment was subcloned into the vector pCATSgfp (kindly provided by Guido Jach, Max-Planck-Institute for Plant Breeding, Germany) digested with *Xho*I and *Nco*I, thereby replacing a translation-enhancing element. This vector contains a codon-optimized GFP S65C mutant gene [17] under the control of the cauliflower mosaic virus CaMV-35S promoter and an additional translation-enhancing element of tobacco etch virus (the basic vector is described in [18]). Transient expression

*Corresponding author. Fax: (49)-221-5062613.

E-mail address: palme@mpiz-koeln.mpg.de (K. Palme).

¹ These authors contributed equally to this study.

Abbreviations: FV, fast-activating vacuolar; SV, slow-activating vacuolar; VK, vacuolar potassium

in tobacco BY2 protoplasts and microscopic analysis were performed as described by Bischoff et al. [19].

2.2. Isolation of the *KCO1::En-1* mutant

The *KCO1::En1* mutant was identified by reverse genetic screening of an *En-1*-mutagenized collection of *Arabidopsis* plants. PCR-based screens were performed as described [20]. The following two primer combinations specific for the *KCO1* gene and the *En-1* transposon were used: (1) *KCO1-14* (5'-CTG CTA GGA CGC CAT TGT TAC CCA CTG AG-3') and *En-8130* (5'-GAG CGT CGG TCC CCA CAC TTC TAT AC-3'); and (2) *En-205* (5'-AGA AGC ACG ACG GCT GTA GAA TAG GA-3') and *KCO1-900* (5'-AGC TGC TTC GAG ATC ATT GTT TGT GAT TC-3').

2.3. RT-PCR

For RT-PCR experiments, total RNA from *Arabidopsis* tissues was isolated using the RNeasy Plant Mini Kit and mRNA was purified twice with the Dynabeads mRNA Direct kit (Dynal, Oslo) to minimize DNA contaminations. Guard-cell and mesophyll protoplasts were prepared as described [21,22] and directly purified with the Dynabeads mRNA Direct kit. First-strand cDNA and quantitative RT-PCR was performed as described before [23] using a LightCycler (Roche). The following K⁺ channel-specific primers were used: *KCO1* fwd (5'-GTT GGC ACG ATT TTC-3'), *KCO1* rev (5'-GCT TCG CAA GAT GAT-3'), *KCO2* fwd (5'-GAT CGG GAC AAA GTG-3'), *KCO2* rev (5'-ACG CAG CCA TTA CAG-3'), *KCO3* fwd (5'-GAC AAT GCG TAT CAG-3'), *KCO3* rev (5'-GCG GTG GTT AAA TCA-3'), *KCO4* fwd (5'-TCA CAT TGC CGA AGA-3'), *KCO4* rev (5'-ACT GCG AAG CCT CTC-3'), *KCO5* fwd (5'-AGA CGA CAA AGA AGA-3'), *KCO5* rev (5'-CCG GTG AGA ATC ATA-3'), *KCO6* fwd (5'-ACC CAA TTC GTC AAA A-3'), *KCO6* rev (5'-CCG CTT AGC AGA GTC T-3'). The GenBank accession numbers are as follows: *KCO1* (X97323), *KCO2* (AJ131641), *KCO3* (AJ010873), *KCO4* (cf. [24]), *KCO5* (AJ243456), *KCO6* (cf. [24]) and *Arabidopsis* actins (cf. [25]). cDNA quantities were calculated by using LIGHTCYCLER 3.5 (Roche). All quantifications were normalized to actin cDNA fragments amplified by *ACT* fwd (5'-GGT GAT GGT GTG TCT-3') and *ACT* rev (5'-ACT GAG CAC AAT GTT AC-3'). To enable detection of contaminating genomic DNA, the primers for *KCO1*, *KCO2* and *KCO3* were selected to flank introns. All kits were used according to the manufacturers' protocols.

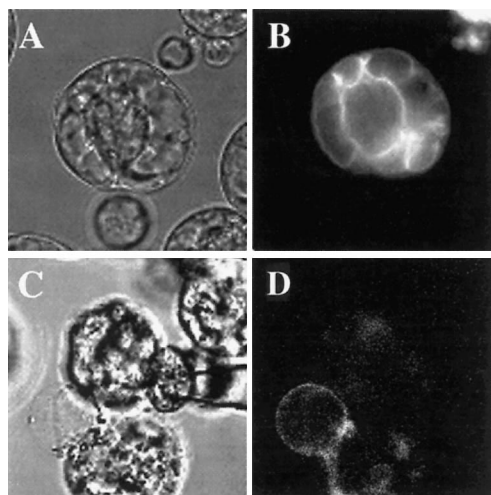


Fig. 1. Images of *KCO1*-GFP fluorescence reveal localization of *KCO1* in the vacuolar membrane. A: Intact tobacco suspension culture cells and the (B) internal *KCO1*-GFP fluorescence of a transfected cell surrounded by non-transfected cells. The transfection rate is usually about 10%. C: A ruptured cell with the vacuole emerging and (D) the corresponding GFP fluorescence recorded with confocal resolution. A,C: Transmission light and (B,D) the same object in fluorescence mode. The emerging vacuole had a diameter of 20 μ m. The tip of the pipette, which was used to rupture the cell, can be seen (C).

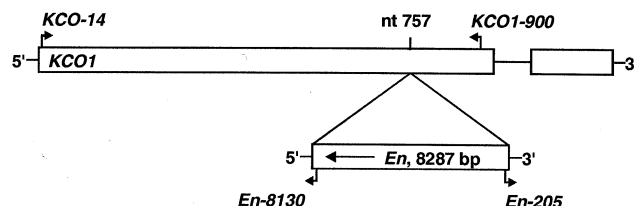


Fig. 2. *Arabidopsis* plant line tagged by *En-1* insertion in the *KCO1* gene (intron indicated as single line). The diagram depicts the insertion and orientation of the transposon in the *KCO1* gene at nucleotide 757. The position and direction of primers are indicated.

2.4. Microscopy

Fluorescent images were taken with a Zeiss Axiovert 135 illuminated at 472 nm by Polychrome II (T.I.L.L. Photonics, Martinsried, Germany) or a Zeiss LSM 410 with a blue (488 nm) argon laser. For the fluorescence channel, a bandpass filter 515–565 nm was used with the 40 \times C-Apochromat water-immersion objective. The *xy*-resolution was set to 0.33 μ m per pixel while the *z*-resolution was about 1.6 μ m.

2.5. Electrophysiology

A. thaliana (Col-0) was grown in a temperature-controlled growth chamber (16 h light, 8 h dark). From protoplasts isolated from mesophyll cells [21], a fresh vacuole was mechanically isolated within the measuring chamber for each patch-clamp measurement [14]. Patch-clamp recordings were performed as described [14]. For recordings on vacuolar membranes, the pipette (vacuolar interior) contained (in mM): 100 KCl, 2 CaCl₂, 5 HEPES/Tris, pH 7.5, adjusted to 400 mOsm with sorbitol. The bathing medium was either the same for recording of SV channels or 2 mM CaCl₂ were substituted by 5 mM EGTA to record FV channels.

3. Results and discussion

3.1. Vacuolar localization of *KCO1*-GFP

Transfected tobacco BY2 protoplasts were identified by the green fluorescence of the expressed *KCO1*-GFP fusion protein. Tobacco cells expressing *KCO1*-GFP show bright staining of vacuolar membranes (Fig. 1A,B). To prove whether *KCO1*-GFP was embedded in the vacuolar membrane, tobacco cells were ruptured to release intact vacuoles (Fig. 1C,D). This was accomplished by either flushing distilled water from a micro-pipette onto the isolated protoplasts [26] or by applying a harsh suction pulse by a patch-pipette filled with bath solution [14]. Images of vacuoles emerging from transfected tobacco cells always showed a pronounced green fluorescence of the vacuolar membrane (Fig. 1D; *n* > 10), indicating that *KCO1* is indeed inserted into this membrane. Vacuolar GFP fluorescence was also detected in epidermal cells following ballistic bombardment of *Arabidopsis* leaves using *CaMV35S::KCO1-GFP* (Meyerhoff, Würzburg, unpublished). Therefore, it is highly unlikely that the observed *KCO1* localization results from mistargeting as frequently observed for plant membrane proteins (e.g. the TIP aquaporins) expressed in heterologous systems [27].

3.2. Isolation of plants carrying an insertion in the *KCO1* gene

To search for an insertion mutant in the *KCO1* gene, we used a reverse genetic approach. Thereby, a transposon-mutagenized *Arabidopsis* population was screened with *KCO1*- and *En-1*-specific primers. We first found an *En-1* transposon located about 1.5 kb upstream of the ATG translational start codon, which can not be expected to cause a strong reduction in mRNA content. In order to obtain a mutant which lacks

KCO1, we screened for an excision–reinsertion event of *En-1*. Among 1800 progeny plants, a single mutant plant (*kco1-7*) was obtained. The transposon had inserted into position nt 757–759, leading to a duplication of Ala₂₅₃, thereby disrupting the open reading frame (Fig. 2). Homozygous progeny of this plant was used for further studies.

3.3. *KCO1* is expressed mainly in mesophyll cells

Quantitative RT-PCR was used to compare *KCO* transcripts between leaves and roots. Thereby, *KCO1* and *KCO6* were found in relatively high concentrations in the leaf only (Fig. 3A). In root, *KCO* transcripts were less abundant. Following enzymatic digestion, mesophyll and guard-cell protoplasts were separated. Mesophyll cells were dominated by *KCO1* and *KCO6* transcripts with a three-fold higher expression level of *KCO1* compared to guard cells (Fig. 3A,B). The number of *KCO6* transcripts in mesophyll cells was four times smaller than that of *KCO1*. In contrast, *KCO6* levels in guard cells were as high as those of *KCO1*. Thus,

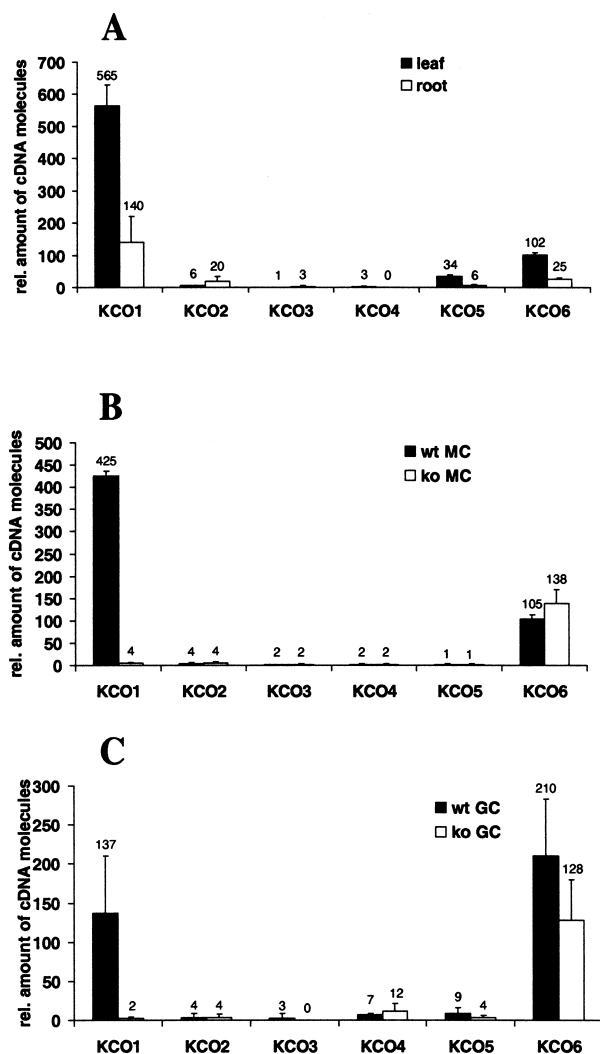


Fig. 3. Expression of *KCO*-type K^+ channels in *Arabidopsis*. A: Expression of *KCO* channels in leaves and roots as determined by quantitative RT-PCR. B: Expression of *KCO1* channels in mesophyll cell (MC) and (C) guard-cell (GC) protoplasts. Numbers of cDNA molecules were normalized with respect to 10 000 molecules of actin ($n=3$; mean \pm S.D.).

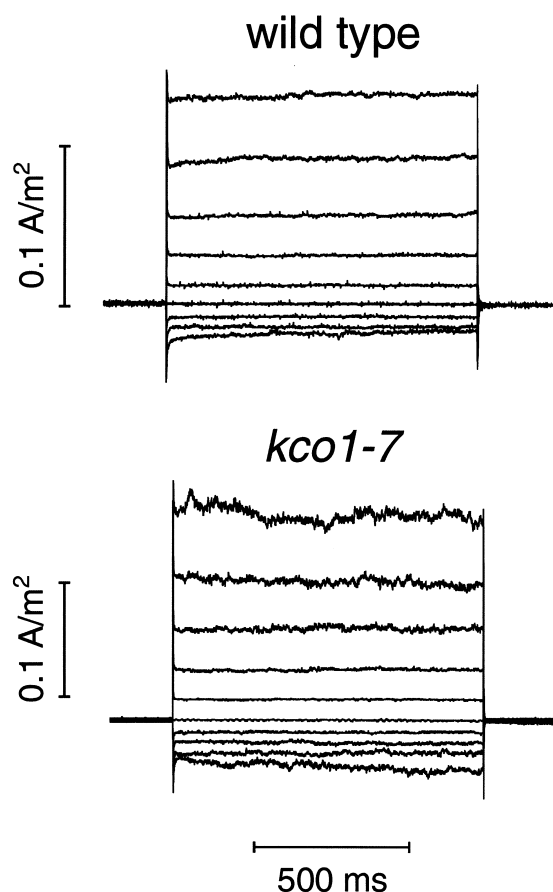


Fig. 4. FV currents of *A. thaliana* mesophyll vacuoles from wild-type (top) and *kco1-7* plants (bottom). From a holding potential of 0 mV, the electrical potential across the tonoplast was changed for 1 s in 20-mV steps from +100 to –60 mV. Current amplitudes were normalized to the vacuolar membrane surface and expressed in A/m². The capacitance of the vacuoles was 67.5 pF (wild-type) and 67.0 pF (*kco1-7*).

KCO1 and *KCO6* are expected to dominate *KCO*-type currents in mesophyll vacuoles. Accordingly, mesophyll vacuoles from *kco1-7* plants should be significantly reduced in the current generated by *KCO1* channels.

3.4. Knockout plants display decreased SV currents

The patch-clamp technique was used to study ion currents of mesophyll vacuoles from *Arabidopsis* wild-type and *kco1-7* plants to address the question whether *KCO1* corresponds to either FV or SV channel activities. Without Ca^{2+} in the bath solution, typical instantaneous outward currents were elicited by positive voltage-pulses. These FV currents did not significantly differ between vacuoles from wild-type and from *kco1-7* plants (Fig. 4). With symmetrical 2 mM Ca^{2+} , characteristic whole-vacuole SV currents became measurable. SV currents recorded from wild-type and *kco1-7* plants appeared qualitatively similar (voltage dependence, kinetics, Ca^{2+} requirement, Fig. 5). When comparing the current densities, however, SV currents from *kco1* plants were smaller than with wild-type vacuoles (Fig. 6). The medians, 2.2 A/m² for the wild-type and 0.55 A/m² for *kco1*, differed by a factor of four, and a *t*-test (of the untransformed data as well as of the logarithmic data) and a Kolmogorov–Smirnov test clearly show that SV current amplitudes from *kco1* plants are significantly smaller than

those from wild-type plants. It should be noted that KCO1 contains a putative 14-3-3 binding site and that this peptide was shown to block the SV channel [28]. This suggests that the KCO1 protein contributes to the formation of functional SV channels. KCO6 transcripts represent 25% when compared to KCO1 (Fig. 3B). Assuming that KCO6 is located in the vacuolar membrane too, it is tempting to speculate that KCO6 accounts for the background SV current in *kco1-7*. Therefore, future studies taking advantage of *kco1-kco6* double mutants together with proteomic approaches to identify the proteins interacting with KCO1 and KCO6 will gain new insights into the role and structure of the SV channel.

Compared to KCO1-mediated whole-cell currents in KCO1 expressing insect cells [16], whole-vacuole SV currents show some similarities but also some striking differences. The SV channel is activated by increasing cytosolic Ca^{2+} but requires higher free Ca^{2+} concentrations and the Ca^{2+} dependence is not as steep [6] as measured with KCO1-expressing insect cells [9,16]. Moreover, increasing vacuolar calcium shifts the voltage dependence of the SV channel in the opposite direction compared to cytosolic Ca^{2+} changes [10,15]. The external concentration of divalent cations, however, does not affect KCO1 [16]. The SV channel hardly discriminates between K^+ and Na^+ [6,26], whereas KCO1 has a six-fold higher permeability for K^+ [16]. In contrast to KCO1, the SV channel is much less sensitive to Ba^{2+} blockage and the block is readily reversible [26,29]. In order to explain these discrepancies, isolated *Arabidopsis* mesophyll vacuoles were analyzed under the same ionic conditions as those originally used for recording

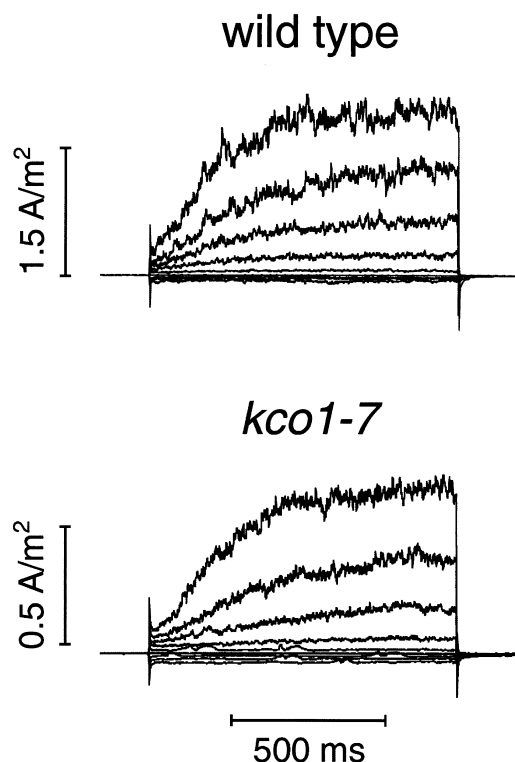


Fig. 5. SV currents of *A. thaliana* mesophyll vacuoles from wild-type (top) and *kco1-7* plants (bottom). Voltage protocol as in Fig. 4. Current amplitudes were normalized to the vacuolar membrane surface and expressed in A/m^2 . Note different scaling of y-axis for wild-type and *kco1-7*. The capacitance of the vacuoles was 5.7 pF (wild-type) and 12.2 pF (*kco1-7*).

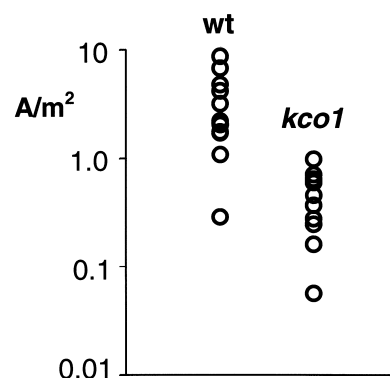


Fig. 6. Comparison of SV current amplitudes in wild-type and *kco1-7* mesophyll vacuoles. Amplitudes of time-dependent currents at +100 mV were normalized to the vacuolar membrane surface and expressed in A/m^2 . Data from 13 vacuoles of seven different wild-type plants are compared with data from 12 vacuoles of eight different *kco1* plants.

KCO1-mediated whole-cell currents in KCO1-expressing insect cells [16]. This was done with the corresponding bath solution in the bath (and the pipette solution in the pipette) as described by Czempinski et al. [16], and, in addition, with bath and pipette solutions reciprocally exchanged. Under both conditions no whole-vacuole currents resembling KCO1-mediated currents [16] could be recorded. It will be interesting to find out why KCO1-mediated K^+ currents recorded in insect cells are so different from vacuolar SV currents.

4. Conclusion

KCO1 is embedded in the vacuolar membrane (Fig. 1). Different *KCO* genes are expressed in leaves, with *KCO1* and *KCO6* showing the highest transcription rates in mesophyll and guard cells (Fig. 3). Disruption (Fig. 2) of KCO1 decreased SV currents of mesophyll by about 75% (Fig. 6), demonstrating that KCO1 contributes to SV currents. The remaining SV currents measured in *kco1* plants (Fig. 5) are most likely due to the expression of *KCO6*.

Acknowledgements: We thank our service group ADIS (Automated DNA Isolation and Sequencing) for DNA sequencing, ZIGIA (Center for Functional Genomics in *Arabidopsis*) for the En lines and support, and Susanne Michel of the central analytics of the SFB 567 for technical assistance. This work was financially supported by the Deutsche Forschungsgemeinschaft (SFB 176, TP B11 and B12), the European Community Biotech program and the International Cooperation Copernicus program.

References

- [1] Schachtman, D.P., Schroeder, J.I., Lucas, W.J., Anderson, J.A. and Gaber, R.F. (1992) *Science* 258, 1654–1658.
- [2] Sentenac, H., Bonneaud, N., Minet, M., Lacroute, F., Salmon, J.M., Gaymard, F. and Grignon, C. (1992) *Science* 256, 663–665.
- [3] Hedrich, R. and Roelfsema, M.R.G. (1999) *Encycl. Life Sci. A* 1307, 1–7.
- [4] Hirsch, R.E., Lewis, B.D., Spalding, E.P. and Sussman, M.R. (1998) *Science* 280, 918–921.
- [5] Ache, P., Becker, D., Ivashikina, N., Dietrich, P., Roelfsema, M.R.G. and Hedrich, R. (2000) *FEBS Lett.* 486, 93–98.
- [6] Hedrich, R. and Neher, E. (1987) *Nature* 329, 833–835.
- [7] Klüsener, B., Boheim, G., Liss, H., Engelberth, J. and Weiler, E.W. (1995) *EMBO J.* 14, 2708–2714.

- [8] Schönknecht, G., Hedrich, R., Junge, W. and Raschke, K. (1988) *Nature* 336, 589–592.
- [9] Reifarth, F.W., Weiser, T. and Bentrup, F.-W. (1994) *Biochim. Biophys. Acta* 1192, 79–87.
- [10] Pottosin, I.I., Tikhonova, L.I., Hedrich, R. and Schönknecht, G. (1997) *Plant J.* 12, 1387–1398.
- [11] Ward, J.M. and Schroeder, J.I. (1994) *Plant Cell* 6, 669–683.
- [12] Hedrich, R., Barbier-Brygoo, H., Felle, H., Flügge, U.-I., Lüttge, U., Maathuis, F.J.M., Marx, S., Prins, H.B.A., Raschke, K., Schnabl, H., Schroeder, J.I., Struve, I., Taiz, L. and Ziegler, P. (1988) *Bot. Acta* 101, 7–13.
- [13] Brüggemann, L.I., Pottosin, I.I. and Schönknecht, G. (1999) *J. Exp. Bot.* 50, 873–876.
- [14] Tikhonova, L.I., Pottosin, I.I., Dietz, K.-J. and Schönknecht, G. (1997) *Plant J.* 11, 1059–1070.
- [15] Allen, G.J. and Sanders, D. (1996) *Plant J.* 10, 1055–1069.
- [16] Czempinski, K., Zimmermann, S., Ehrhardt, T. and Müller-Röber, B. (1997) *EMBO J.* 16, 2565–2575.
- [17] Heim, R., Cubitt, A.B. and Tsien, R.Y. (1995) *Nature* 373, 663–664.
- [18] Carrington, J.C. and Freed, D.D. (1990) *J. Virol.* 64, 1590–1597.
- [19] Bischoff, F., Vahlkamp, L., Molendijk, A. and Palme, K. (1999) *Plant Mol. Biol.* 42, 515–530.
- [20] Baumann, E., Lewald, J., Saedler, H., Schulz, B. and Wisman, E. (1998) *Theor. Appl. Genet.* 97, 729–734.
- [21] Sando, S. and Goto, N. (1994) *Plant Cell Rep.* 14, 75–80.
- [22] Hedrich, R., Busch, H. and Raschke, K. (1990) *EMBO J.* 9, 3889–3892.
- [23] Szyroki, A., Ivashikina, N., Dietrich, P., Roelfsema, M.R., Ache, P., Reintanz, B., Deeken, R., Godde, M., Felle, H., Steinmeyer, R., Palme, K. and Hedrich, R. (2001) *Proc. Natl. Acad. Sci. USA* 98, 2917–2921.
- [24] Mäser, P., Thomine, S., Schroeder, J.I., Ward, J.M., Hirschi, K., Sze, H., Talke, I.N., Amtmann, A., Maathuis, F.J., Sanders, D., Harper, J.F., Tchieu, J., Gribskov, M., Persans, M.W., Salt, D.E., Kim, S.A. and Guerinot, M.L. (2001) *Plant Physiol.* 126, 1646–1667.
- [25] An, Y.Q., McDowell, J.M., Huang, S., McKinney, E.C., Chambliss, S. and Meagher, R.B. (1996) *Plant J.* 10, 107–121.
- [26] Schulz-Lessdorf, B. and Hedrich, R. (1995) *Planta* 197, 655–671.
- [27] Maurel, C., Reizer, J., Schroeder, J.I. and Chrispeels, M.J. (1993) *EMBO J.* 12, 2241–2247.
- [28] van den Wijngaard, P.W.J., Bunney, T.D., Roobeek, I., Schönknecht, G. and de Boer, A.H. (2000) *FEBS Lett.* 488, 100–104.
- [29] Hedrich, R. and Kurkdjian, A. (1988) *EMBO J.* 7, 3661–3666.